Pain 114 (2005) 429–443

PAIN

www.elsevier.com/locate/pain

New evidence that both T-type calcium channels and $GABA_A$ channels are responsible for the potent peripheral analgesic effects of 5α-reduced neuroactive steroids

Sriyani Pathirathna[a], Barbara C. Brimelow[a], Miljen M. Jagodic[a], Kathiresan Krishnan[b], Xin Jiang[b], Charles F. Zorumski[c], Steven Mennerick[c], Douglas F. Covey[b], Slobodan M. Todorovic[a], Vesna Jevtovic-Todorovic[a,*]

[a]*Department of Anesthesiology, University of Virginia Health System, Charlottesville, VA, USA*
[b]*Department of Molecular Biology and Pharmacology, Washington University School of Medicine, St Louis, MO, USA*
[c]*Department of Psychiatry, Washington University School of Medicine, St Louis, MO, USA*

Received 1 June 2004; received in revised form 5 November 2004; accepted 14 January 2005

Abstract

Neurosteroids are potent blockers of neuronal low-voltage activated (T-type) Ca^{2+} channels and potentiators of $GABA_A$ ligand-gated channels, but their effects in peripheral pain pathways have not been studied previously. To investigate potential analgesic effects and the ion channels involved, we tested the ability of locally injected 5α-reduced neurosteroids to modulate peripheral thermal nociception to radiant heat in adult rats in vivo and to modulate $GABA_A$ and T-type Ca^{2+} channels in vitro. The steroid anesthetic alphaxalone (ALPX), the endogenous neurosteroid allopregnanolone (3α5αP), and a related compound ((3α,5α,17β)-3-hydroxyandrostane-17-carbonitrile, (ACN)), induced potent, dose-dependent, enantioselective anti-nociception in vivo and modulation of both T-type Ca^{2+} currents and $GABA_A$-mediated currents in vitro. Analgesic effects of ALPX were incompletely antagonized by co-injections of the $GABA_A$ receptor antagonist bicuculline. The neurosteroid analogue ((3α,5α)-3-hydroxy-13,24-cyclo-18,21-dinorchol-22-en-24-ol (CDNC24), a compound with GABAergic but not T-type activity, was not analgesic. However, (3β,5α,17β)-17-hydroxyestrane-3-carbonitrile (ECN)), which has effects on T-type channels but not on $GABA_A$ receptors, also induced potent enantioselective peripheral anti-nociception. ECN increased pain thresholds less than ALPX, 3α5αP and ACN. However, when an ineffective dose of CDNC24 was combined with ECN, anti-nociceptive activity was greatly enhanced, and this effect was bicuculline-sensitive. These results strongly suggest that $GABA_A$ channels do not contribute to baseline pain transmission, but they can enhance anti-nociception mediated by blockade of T-type Ca^{2+} channels. In conclusion, we demonstrate that potent peripheral analgesia induced by 5α-reduced neurosteroid is mediated in part by effects on T-type Ca^{2+} channels. Our results also reveal a role of GABA-gated ion channels in peripheral nociceptive signaling.

Keywords: Adult rats; Thermal anti-nociception; T-channel blockers; Dorsal root ganglia; Peripheral nociceptors

1. Introduction

Neuroactive steroids modulate the function of many ligand- and voltage-gated ion channels with much of the attention focused on their modulation of $GABA_A$ receptor function (Lambert et al., 1995; Zorumski et al., 2000). We previously reported that the novel neuroactive steroid, ECN ((3β,5α,17β)-17-hydroxyestrane-3-carbonitrile, Fig. 1), is a potent and enantioselective blocker of T-type Ca^{2+} channels in rat sensory neurons (IC_{50} 300 nM for ECN; IC_{50} 8.8 μM for *ent*-ECN), and unlike many other neuroactive steroids does not affect $GABA_A$ currents in hippocampal neurons (Todorovic et al., 1998). In addition, some other 5α-reduced neuroactive steroids such as ALPX ((3α,5α,)-3-hydroxypregnane-11,20-dione) and ACN ((3α,5α,17β)-3-hydroxyandrostane-17-carbonitrile) are potent blockers of T currents in dissociated small size rat

* Corresponding author. Tel.: +1 434 924 2283; fax: +1 434 982 0019.
E-mail address: vj3w@virginia.edu (V. Jevtovic-Todorovic).

0304-3959/$20.00
doi:10.1016/j.pain.2005.01.009

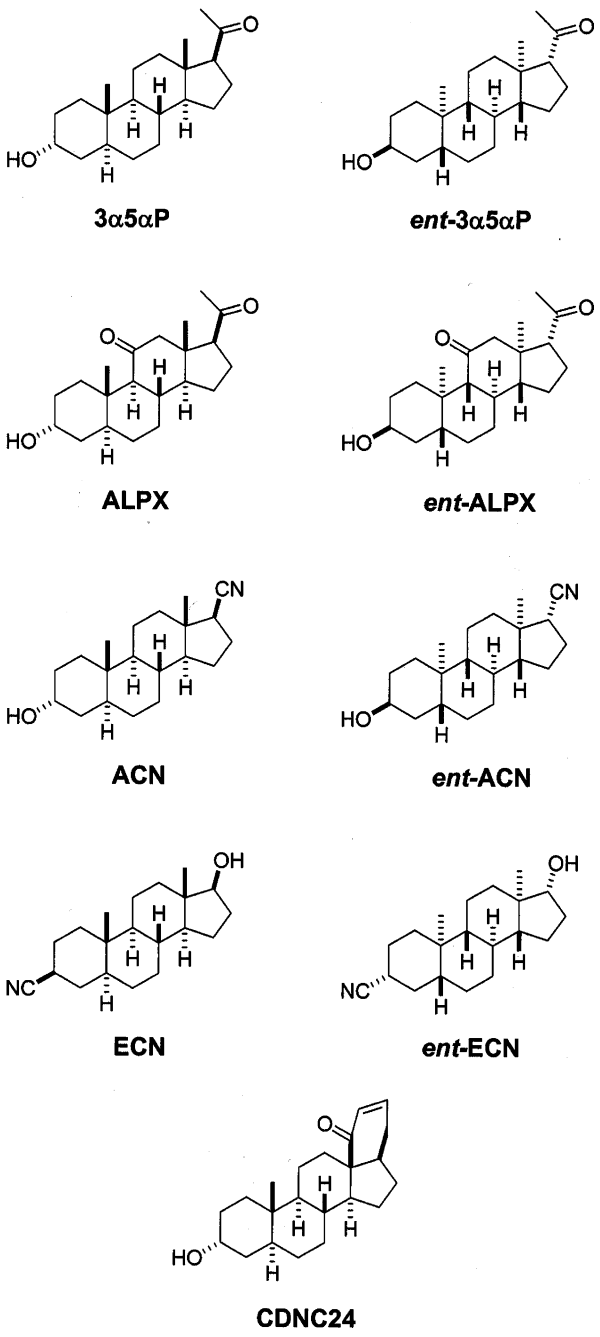

Fig. 1. Chemical structures of 5α-reduced neuroactive steroids used in this study.

sensory neurons (most of which are nociceptors) suggesting that T-channels might be an important cellular target for a variety of neuroactive steroids (Todorovic et al., 1998).

T-type (low voltage-activated, LVA) Ca^{2+} channels have been identified in a variety of excitable and non-excitable cells (Carbone and Lux, 1984; White et al., 1989; Perez-Reyes, 2003). While the important role of high voltage-activated (HVA) Ca^{2+} channels in synaptic transmission is well established, the function of T-channels remains less certain. Since T-channels act over a range of membrane potentials near the resting potential of most cells, they are thought to play a crucial role in controlling cellular excitability under physiological and pathological conditions (Huguenard, 1996; Ertel et al., 1997; Perez-Reyes, 2003).

Although T-currents are relatively easy to study in vitro due to their unique biophysical properties, study of their function in vivo is hampered by a lack of selective pharmacological agents. Thus, despite their presence in nociceptive neurons (Schroeder et al., 1990; Cardenas et al., 1995), the functional role of T-type Ca^{2+} channels in sensory processing remains poorly understood. However, some promising clues have begun to emerge. Recently, the important role of T-type Ca^{2+} channels in somatic (Todorovic et al., 2001) and visceral peripheral nociception (Kim et al., 2003) has been reported. These studies and others (Dogrul et al., 2003) are creating interest in exploring the therapeutic potential of T-type Ca^{2+} current modulation for pain treatment.

Because T-channels in the peripheral nerve endings of skin may act as the amplifiers of nociceptive transmission in vivo (Todorovic et al., 2001), we proposed that 5α-reduced neuroactive steroids that are potent T-type Ca^{2+} channel blockers in vitro might be effective peripheral analgesics in vivo. To test this hypothesis we examined a series of steroid analogs that were either synthesized by us (ACN, *ent*-ACN, ECN, *ent*-ECN, CDNC24, *ent*-3α5αP and *ent*-ALPX) or purchased commercially (ALPX and 3α5αP) for their effects in vitro on T current in acutely dissociated sensory neurons from dorsal root ganglia or on rat α1β2γ2L type $GABA_A$ receptors expressed in *Xenopus laevis* oocytes and in vivo on peripheral thermal nociception following local injection into the peripheral receptive fields of a rat hind paws (Todorovic et al., 2001, 2002). The neuroactive steroids were divided into three groups based on their actions: one group had a selective potentiating effect on $GABA_A$ current (CDNC24), a second group had a selective blocking effect on T-type voltage-gated Ca^{2+} current (ECN and *ent*-ECN) and the third group had both effects (ACN, *ent*-ACN, ALPX, *ent*-ALPX, 3α5αP and *ent*-3α5αP). The selective pharmacological actions of this collection of neuroactive steroids provided a unique opportunity to compare and contrast the role of these two distinct families of ion channels in peripheral somatic nociception.

2. Methods

2.1. In vivo studies

All experimental protocols were approved by the University of Virginia Animal Care and Use Committee, Charlottesville, VA. Every effort was made to minimize animal suffering and the number of animals used.

2.1.1. Chemicals and animals

Adult Sprague–Dawley female rats (weight 300–330 g) were used for all in vivo experiments because female rats are less aggressive and easier to handle during pain testing. ALPX and 3α5αP were obtained from Sigma Chemical Company (St. Louis, MO). ACN, *ent*-ACN, *ent*-3α5αP and CDNC24 were prepared as described previously (Hu et al., 1993;1997; Jiang et al., 2003). ECN was prepared from 19-nortestosterone by initial acetylation of the 17-hydroxyl group, conversion of the 3-ketone group into the epimeric 3-carbonitriles (separated by chromatography), and removal of the 17-acetate group using the methods described earlier for the preparation of neurosteroids containing the 17-carbonitrile group (Han et al., 1996). The *ent*-ECN was prepared from *ent*-19-nortestosterone using the same procedure. The *ent*-19-nortestosterone and *ent*-ALPX were prepared by total synthesis from 2-methyl-1,3-cyclopentanedione using modifications of the synthetic procedures reported previously for the total synthesis of *ent*-3α5αP (Hu et al., 1997). The total synthesis of *ent*-ECN and *ent*-ALPX will be described elsewhere. All synthesized compounds were chromatographically pure and had spectroscopic data (IR, NMR) consistent with the assigned structures and were shown to have the correct elemental composition by combustion analysis for C, H, and when present, N. Optical rotations of the *ent*-steroids were, within the limits of experimental error, equal and opposite to those of the corresponding steroid.

All steroids were dissolved in DMSO and later diluted in saline so that the final DMSO concentration did not exceed 3% (at this concentration DMSO did not have any effect on paw withdrawal latency in rats—data not shown).

2.1.2. Assessment of thermal nociception

Nociceptive responses to thermal stimulation were measured using a paw thermal stimulation system consisting of a clear plastic chamber (10×20×24 cm) that sits on an elevated clear glass floor and is temperature regulated at 30 °C (Hargreaves et al., 1988; Jevtovic-Todorovic et al., 1998, 2003). Each animal was placed in the plastic chamber to accommodate for 15 min. A radiant heat source mounted on a movable holder beneath the glass floor was positioned to deliver a thermal stimulus to the plantar side of the hind paw. When the animal withdraws the paw, a photocell detects interruption of a light beam reflection and the automatic timer shuts off. This method has a precision of ±0.05 s for the measurement of paw withdrawal latency (PWL). To prevent thermal injury, the light beam automatically discontinued at 20 s if the rat failed to withdraw its paw.

To test the effects of neuroactive steroids when administered into the peripheral receptive fields, we injected 100 μL of test compound intradermally in the ventral side of the right hind paw. The non-injected side (left hind paw) was used as a control in each animal. All solutions were pH balanced to 7.4 to avoid skin irritation. There were no signs of skin inflammation, discoloration or irritation at the site of injection with test compounds. All doses are expressed in μg per 100 μL. At 10, 20 and 60 min after drug administration, the thermal stimulus was applied and PWLs were measured. The investigator assessing behavior was kept unaware of the pharmacological interventions.

2.1.3. Statistical analysis

Analysis of variance (ANOVA) was used to compare the effects of neuroactive steroids or vehicle treatment on thermal nociception; PWL measured during thermal nociceptive testing was the dependent variable. To evaluate the course of thermal nociception during drug/vehicle treatment, comparisons were conducted between injected (right) paw vs. non-injected (left paw) PWLs across all of the post-treatment test sessions (i.e. 10, 20 and 60 min post-treatment). Effects of drug treatments on thermal nociception were also evaluated by conducting a one-way, repeated measures ANOVA on the PWLs measured during the pretreatment on the injected paw (baseline-B) and all the post-treatment tests. Subsequent pairwise comparisons between the pre- and post-treatment PWLs were conducted if significant F values resulted from one-way ANOVA and alpha levels were adjusted using the Bonferroni procedure when appropriate.

Dose–response data were fit to the function

$$\mathrm{PI}([\mathrm{NEUROSTEROID}]) = \mathrm{PI}_{\max}/(1 + (\mathrm{ED}_{50}/[\mathrm{NEUROSTEROID}])^{n})$$

where $\mathrm{PI}_{\max}$ is the maximal increase in PWLs caused by a drug in the injected vs. non-injected paw 10 min post-injection; the ED_{50} is the dose that produces half-maximal increase in PWLs indicating an analgesic effect; and n is the apparent Hill coefficient indicating the slope of the curve. Fitted values are reported with 95% linear confidence limits. Fitting was done with Origin 7.0 software (OriginLab Corp., Northhampton, MA).

2.2. In vitro studies

2.2.1. Electrophysiological methods, solutions and current isolation procedures

Acutely dissociated dorsal root ganglia (DRG) neurons from adult male Sprague–Dawley rats (100–300 g) were obtained using enzymatic treatment and standard whole cell patch-clamp techniques as described elsewhere (Todorovic and Lingle, 1998; Todorovic et al., 1998). Glass coverslips with adherent DRG cells were transferred to a standard culture dish with a total volume <1 mL. The solution application system consisted of multiple, independently controlled glass capillary tubes, while solution was removed from the opposite end of the chamber by constant suction. Manually controlled valves accomplished switching between solutions. Test solutions were maintained in all-glass syringes and allowed to flow by gravity. Use of glass syringes and capillary tubes minimized loss of lipophilic steroid compounds during perfusion. Changes in Ca^{2+} current amplitude in response to rapidly acting drugs or ionic changes were typically complete in 10–20 s. Switching between separate perfusion syringes, each containing control saline, resulted in no changes in Ca^{2+} current.

Most data from DRG cells were obtained from smaller diameter neurons with no visible processes. Voltage commands and digitization of membrane currents were done with Clampex 8.2 of the pClamp software package (Axon Instruments, Foster City, CA) running on an IBM-compatible computer. Membrane currents were recorded with an Axopatch 200A patch-clamp amplifier (Axon Instruments). Reported series resistance and capacitance values were taken from the reading of the amplifier. The average uncompensated (series resistance) R_s was 7±3 (mean±SD) MΩ, and the average membrane capacitance (C_m) was 14±4 pF in the 61 neurons studied. These were typically compensated 40–80% without oscillation in current traces. To record T-currents, neurons were held at −90 mV and stepped to −30 mV to evoke inward currents that inactivate almost completely during a 200 ms test

pulse. The intracellular saline for recording T-currents consisted (in mM) of: 135–140 TMAOH, 10 ethylene-glycol-bis-(β-aminoethyl ether) *N*,*N*,*N*′,*N*′-tetraacetic acid (EGTA), 40 HEPES, and 2 $MgCl_2$, titrated to pH 7.15–7.20 with HF. In the presence of intracellular F^-, L-type HVA currents were substantially reduced (Todorovic and Lingle, 1998) while N-type HVA currents were blocked by pre-incubation in 1 μM ω-CgTx-GVIA. Because of the possibility of some residual HVA current contamination, all measurements of T-current amplitude in DRG cells were made from the peak of the inward current to the current remaining at the end of a 200 ms test step. The standard extracellular saline for recording T-type Ca^{2+} currents contained (in mM): 152 tetraethylammonium (TEA)-Cl, 10 HEPES and 10 $BaCl_2$, adjusted to pH 7.4 with TEA-OH, osmolarity 316 mOsm. All steroids were dissolved in DMSO to make 10–30 mM stock solutions. Aliquots of the stock solutions were added to the standard external solution to achieve final concentrations stated in the text. The final concentration of DMSO was less than 0.6% in these experiments; this concentration of DMSO did not affect I_{Ba} (data not shown, $n=5$).

Voltage-gated Na^+ currents and voltage-gated K^+ currents were recorded as reported previously (Todorovic et al., 2001). On establishing whole-cell configuration, a series resistance compensation of 75% was applied and cells were held at −90 mV. Cells that showed evidence of poor voltage control, as reflected by the shape of the current–voltage curve, were excluded from the study.

The standard external solution for recording voltage-gated K^+ currents contained (in mM): 140 NaCl, 5 KCl, 2 $MgCl_2$, 2.0 $CaCl_2$, 10 glucose and 10 HEPES, pH 7.4 with NaOH. The standard pipette solution used to record voltage-gated K^+ currents contained (in mM): 110 KCl, 14 phosphocreatine, 10 HEPES, 9 EGTA, 5 Mg-ATP and 0.3 Tris-GTP, 2 mM QX 314, pH adjusted to 7.2 with CsOH. To record voltage-gated K^+ currents cells were held at −60 mV and depolarized to +60 mV by a 150 ms depolarizing step. Extracellular solution for recording of voltage-gated Na^+ currents was same as for recording of K^+ currents (0.2 mM $CdCl_2$ added to block voltage-gated Ca^{2+} currents) and internal solution was same as for recording of T currents. Voltage-gated Na^+ currents were evoked with voltage steps from −90 to −30 mV using a 20 ms depolarizing step.

2.2.2. Analysis of Ca^{2+} current blockade

The percent reduction in peak inward current carried by barium ions at a given steroid concentration was used to generate concentration–response curves. For each of these curves, all points are averages of multiple determinations obtained from at least five different cells. On all plots vertical bars indicate standard errors. Mean values on all concentration–response curves were fit to the following function

$$\mathrm{PB}([\mathrm{Neurosteroid}]) = \mathrm{PB}_{\max}/(1 + (\mathrm{IC}_{50}/[\mathrm{Neurosteroid}])^n)$$

where PB_{max} is the maximal percent block of peak T current, IC_{50} is the concentration that produces 50% of maximal inhibition, and n is the apparent Hill coefficient for blockade.

Fitted values are typically reported with 95% linear confidence limits.

The voltage-dependence of steady-state activation and inactivation was described by the Boltzmann distribution

$$I(V) = I_{\max}/(1 + \exp[-(V - V_{50})/k])$$

where I_{max} represents maximal activatable current, V_{50} represents the voltage where half of the current is activated or inactivated, and k (units of millivolts) represents the voltage dependence of distribution.

2.2.3. Xenopus oocyte expression studies

Stage V–VI oocytes were harvested from sexually mature female *X. laevis* (Xenopus One, Northland, MI) under 0.1% tricaine (3-aminobenzoic acid ethyl ester) anesthesia, according to institutionally approved protocols. Oocytes were defolliculated by shaking for 20 min at 37 °C in collagenase (2 mg/mL) dissolved in calcium-free solution containing (in mM): 96 NaCl, 2 KCl, 1 $MgCl_2$, and 5 HEPES at pH 7.4. Capped mRNA, encoding rat $GABA_A$ receptor α1, β2 and γ2L subunits was transcribed in vitro using the mMESSAGE mMachine Kit (Ambion, Austin, TX) from linearized pBluescript vectors containing receptor coding regions. Subunit transcripts were injected in equal parts (20–40 ng total RNA) 8–24 h following defolliculation. Oocytes were incubated up to 5 days at 18 °C in ND96 medium containing (in mM): 96 NaCl, 1 KCl, 1 $MgCl_2$, 2 $CaCl_2$ and 10 HEPES at pH 7.4, supplemented with pyruvate (5 mM), penicillin (100 U/mL), streptomycin (100 μg/mL) and gentamycin (50 μg/mL).

2.2.4. Oocyte electrophysiology

Two-electrode voltage-clamp experiments were performed with a Warner OC725 amplifier 2–5 days following RNA injection. The extracellular recording solution was ND96 medium with no supplements. Intracellular recording pipettes were filled with 3 M KCl and had open tip resistances of ∼1 MΩ. Drugs were applied from a common tip via a gravity-driven multibarrel drug-delivery system. Cells were clamped at −70 mV for all experiments, and unless otherwise noted, the current at the end of 20–30 s drug applications was measured for quantification of current amplitudes. Steroids were prepared in a DMSO stock at 10–100 mM and diluted so that the final concentration of DMSO was less than 0.5%. At this concentration, DMSO had no effect on GABA responses.

3. Results

To establish a reference for comparing the analgesic effects of synthesized neuroactive steroids, our initial in vitro (Figs. 2 and 3) and in vivo (Fig. 4) experiments focused on the endogenous neurosteroid, 3α5αP. 3α5αP potentiates $GABA_A$-induced currents in vitro (Majewska et al., 1986; Callachan et al., 1987; Wittmer et al., 1996), and here we show that 3α5αP also blocks T-type Ca^{2+} currents. Fig. 2 summarizes the effects of 3α5αP on inward T currents recorded from acutely dissociated rat sensory neurons. 3α5αP induced partial (maximal decrease about 45%) (Fig. 2A), but potent blockade of T-currents (calculated IC_{50} was 0.9 ± 0.4 μM). Furthermore, block of T currents was strongly enantioselective with *ent*-3α5αP being about 20 times less potent (IC_{50} 18.6 ± 0.2 μM) with similar maximal block as depicted in Fig. 2C and D.

We next determined whether 3α5αP alters the kinetic properties of T currents. Fig. 3A depicts a family of inward currents evoked from a holding potential of −90 mV to

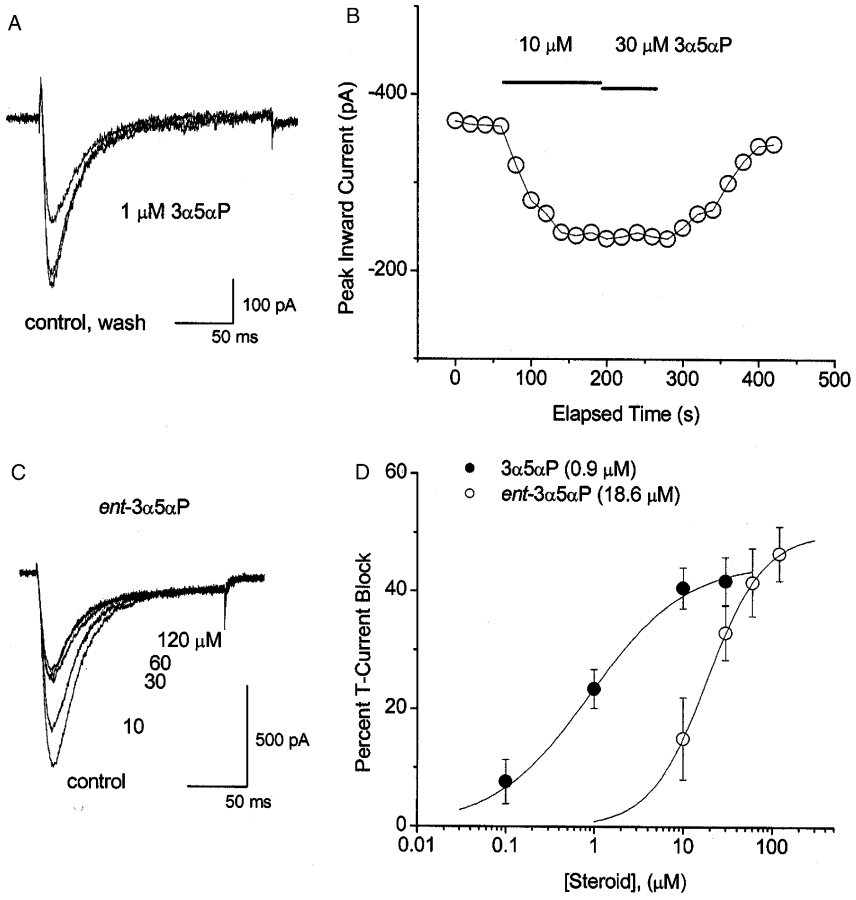

Fig. 2. The effects of 3α5αP and *ent*-3α5αP on T currents in small size rat sensory neurons. (A) The panel depicts traces from an experiment where 1 μM 3α5αP reversibly blocked about 30% of the peak inactivating inward Ca^{2+} currents elicited by membrane depolarization from −90 to −35 mV. Bars indicate calibration. (B) The graph shows the time course of T-current blocking effect of 3α5αP in another DRG neuron. Horizontal bars indicate times of drug application. Ten micromolar 3α5αP blocked about 40% of the peak inward current; addition of 30 μM of 3α5αP did not induce more profound blockade of T current. (C) The traces depict the dose–response effect of several concentrations of *ent*-3α5αP on T currents. (D) The graph shows the concentration-dependent blockade of T currents by 3α5αP and *ent*-3α5αP at holding potentials of −90 mV. Points represent averages of at least five different cells, vertical lines represent standard errors (SE) and solid line is the best fit of Hill plot yielding an IC_{50} value of 0.9±0.2 μM with Hill coefficient of 0.8±0.1, and maximal block of 45±3% (total of 12 cells) for 3α5αP and an IC_{50} value of 18.6±0.2 μM with Hill coefficient of 1.4±0.1, and maximal block of 50±0.5% (total of nine cells) for *ent*-3α5αP.

−60 to +60 mV in the absence (upper panel) and presence (lower panel) of 10 μM 3α5αP. 3α5αP did not significantly alter the time course of T current activation, measured as 10–90% rise time, or inactivation (n=4 cells per data point), measured by the fit of a single exponential function to the decaying phase of the current at potentials from −50 to −10 mV. Fig. 3B depicts an average current–voltage curve from four cells in the absence (filled symbols) and presence of 10 μM 3α5αP (open symbols).

Because many blockers of ion channels exhibit voltage-dependent features, we examined whether 3α5αP alters voltage-dependent inactivation of T-channels at different potentials. T currents were evoked by a voltage step to −30 mV after 5 s conditioning step at potentials from −110 to −40 mV in the presence and absence of 10 μM 3α5αP (Fig. 3C). This protocol defines the voltage-dependence of T current fractional availability in rat sensory neurons (Todorovic and Lingle, 1998). The normalized maximal current elicited from each conditioning potential is plotted as a function of the conditioning potential (Fig. 3D) (n=4 cells). Based on the best fits using the Boltzmann equation, we found that, under control conditions, half availability (V_{50}) occurred at −76 mV with a slope factor of 7.2 mV. However, in the presence of 3α5αP, V_{50} occurred at −86 mV with a slope factor of 6.9 mV, thus shifting the steady state inactivation to more negative potentials. These experiments indicate that 3α5αP and other 5α-reduced neuroactive steroids (Todorovic et al., 1998) exert more prominent blocking effects on T currents at more positive conditioning potentials, presumably by stabilizing inactive states of the channel. Consistent with a mild voltage-dependent blockade of T current, both 3α5αP and *ent*-3α5αP were slightly more potent at more depolarized holding potentials such as −70 mV (Fig. 3F). On the other hand, there was very little effect of 3α5αP on the voltage dependence of activation (n=4 cells, Fig. 3E). In other experiments, application of

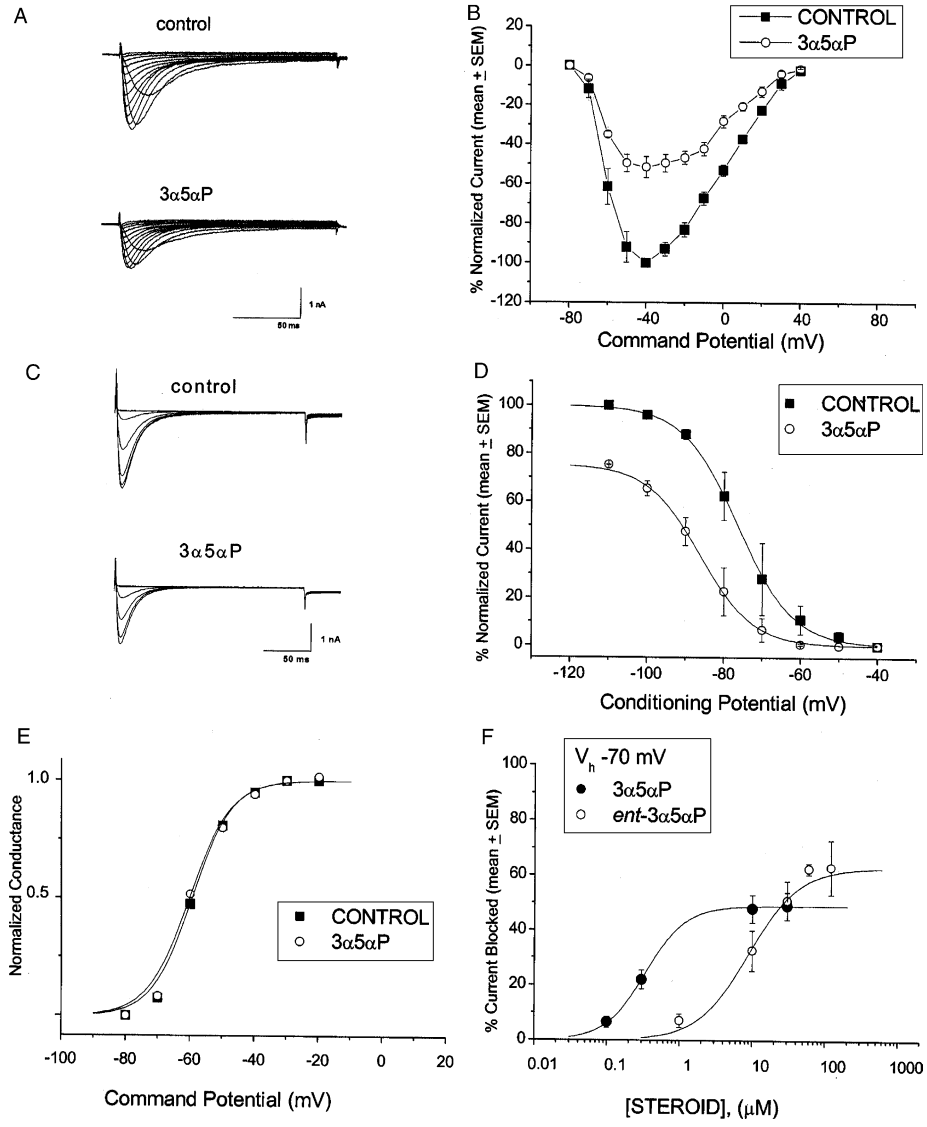

Fig. 3. Mechanisms of block of T currents in DRG neurons by 3α5αP. (A) Traces from an experiment showing the effects of 10 μM 3α5αP on a family of well-isolated T currents evoked from −90 mV to test potentials from −60 to +60 mV. (B) Averaged current–voltage curves from four cells in control (filled squares) and in the presence of 10 μM 3α5αP (open circles) where similar experiments were performed as depicted in panel A of this figure. (C) Traces of T currents obtained using a paired-pulse protocol to study steady-state inactivation in the absence and in the presence of 3α5αP in the same DRG neuron as depicted in panel A of this figure. (D) The steady-state inactivation curves obtained in the absence (filled squares) and presence of 10 μM 3α5αP (open circles) show a shift of 10 mV in the hyperpolarizing direction by steroid ($n=4$ cells). The solid lines are the best fit of the Boltzmann distribution with a calculated V_{50} of -76.0 ± 0.3 mV and a slope factor of 7.2 ± 0.2 mV in control conditions. The V_{50} in the presence of 10 μM 3α5αP was -86.0 ± 0.3 mV, with a slope factor of 6.9 ± 0.3 mV. (E) 3α5αP has very little effect on the voltage-dependence of T current activation in DRG cells. This graph shows apparent peak conductance values defined as $I_{peak}/(V-E_r)$ plotted against command potentials. The extrapolated reversal potential (E_r) was taken to be +50 mV. Estimates of V_{50} and k show only small shifts with even up to 20 mV differences in assumed reversal potential values. The best fit of the Boltzmann equation in the absence of steroid (filled symbols) showed half-maximal activation at -59.5 ± 0.8 mV with a slope factor of 6.2 ± 0.8 mV ($n=4$ cells per data point). In the presence of 10 μM 3α5αP (open circles), half-maximal activation was -60.3 ± 1.2 mV and slope factor was 6.4 ± 1.1 mV. (F) The graph shows the concentration-dependent blockade of T currents by 3α5αP and *ent*-3α5αP at holding potential of −70 mV. Points represent averages of at least five different cells, vertical lines represent standard errors (SE) and solid line is the best fit of the Hill equation with an IC_{50} value of 0.75 ± 0.30 μM, a Hill coefficient of 0.78 ± 0.20, and maximal block of $50\pm7\%$ (total of seven cells) for 3α5αP and an IC_{50} value of 9.0 ± 1.6 μM with a Hill coefficient of 1.25 ± 0.26 and maximal block of $63\pm10\%$ (total of eight cells) for *ent*-3α5αP.

10 μM 3α5αP had very little effect on total voltage-gated Na^+ currents ($1\pm1\%$ change, $P>0.05$, $n=5$, data not shown) and voltage-gated K^+ currents ($1\pm2\%$ change, $n=4$, $P>0.05$, data not shown).

In vivo, 3α5αP induced dose-dependent and potent peripheral analgesia when injected locally into peripheral receptive fields of sensory neurons (Fig. 4A, upper panel). Significant analgesia was achieved with very low doses of 3α5αP (as low as 0.01 μg/100 μL). The highest dose (1 μg/100 μL) induced profound analgesia (an increase in thermal PWLs of about 6 s when compared to non-injected paw) that lasted at least for 20 min. Stable PWLs recorded from

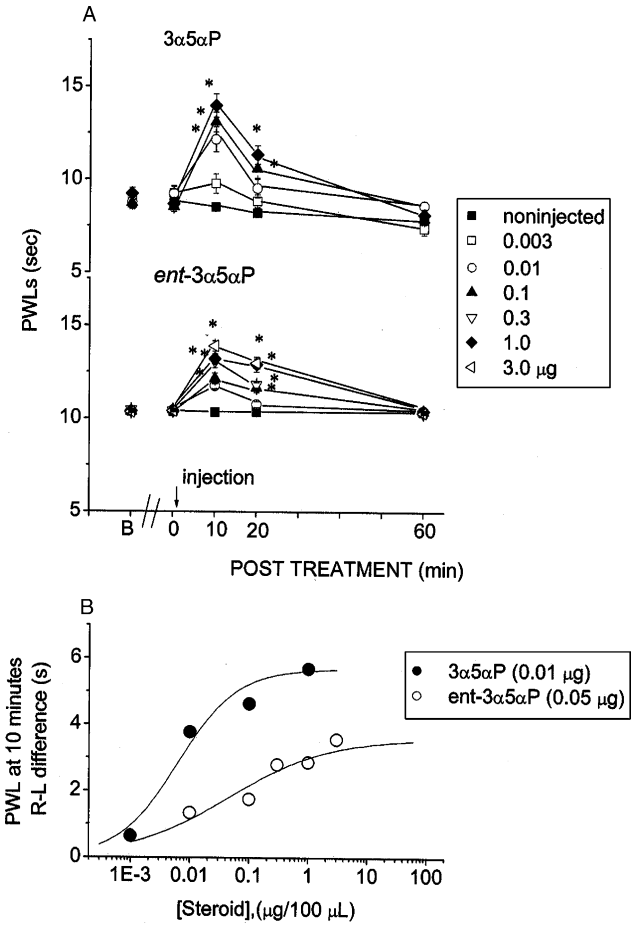

Fig. 4. 3α5αP is a potent and enantioselective peripheral analgesic. (A) *Upper panel*—Injection of 3α5αP induces a dose-dependent increase in thermal PWLs when compared to non-injected paws. At 0.01, 0.1 and 1.0 μg/100 μL, 3α5αP significantly increased PWLs [*, $F(1,22)=64.37$, $P<0.0001$; $F(1,22)=63.12$, $P<0.0001$; $F(1,22)=71.88$, $P<0.0001$, respectively] at 10 min and the two highest doses (0.1 and 1.0 μg/100 μL) significantly increased PWLs [*, $F(1,22)=17.11$, $P<0.0001$; $F(1,22)=29.27$, $P<0.0001$, respectively] at 20 min post-injection when compared to the non-injected paw (closed squares). PWLs returned to control values by 60 min following injection ($n=9$–12 animals per time point). *Lower panel*—Injection of *ent*-3α5αP induces a dose-dependent increase in thermal PWLs when compared to non-injected paws. At 0.01, 0.1, 0.3, 1.0 and 3.0 μg/100 μL, *ent*-3α5αP significantly increased PWLs [*, $F(1,4)=11.19$, $P<0.001$; $F(1,4)=10.29$, $P<0.001$; $F(1,4)=14.82$, $P=0.001$; $F(1,4)=13.09$, $P<0.001$, $F(1,4)=22.65$, $P<0.001$, respectively] at 10 min and at 0.1, 0.3, 1.0 and 3.0 μg/100 μL significantly increased PWLs [*, $F(1,4)=7.22$, $P<0.001$; $F(1,4)=7.69$, $P<0.001$; $F(1,4)=11.84$, $P<0.001$; $F(1,4)=16.58$, $P<0.001$, respectively] at 20 min post-injection when compared to the non-injected paw (closed squares). PWLs returned to control values by 60 min following injection ($n=9$–12 animals per time point). (B) Dose-dependent thermal analgesia following local injection of 3α5αP (closed circles) and *ent*-3α5αP (open circles). Average dose–response curves for local analgesia are based on the maximal increase in thermal PWLs on injected paw (right) vs. non-injected (left) paw 10 min after injection (the maximal effect) (*y*-axis) and dose of 3α5αP or *ent*-3α5αP expressed in μg/100 μL (*x*-axis). Solid lines are best fits of the Hill equation (see Section 2). Fits were constrained to maximal increase in PWLs of 5.7 and 3.6 s with $ED_{50}=0.01\pm0.002$ and 0.05 ± 0.02 μg, Hill coefficient 0.9 ± 0.3 and 0.5 ± 0.1 for 3α5αP and *ent*-3α5αP, respectively.

the non-injected contra-lateral paw indicate lack of a systemic effect. Like the in vitro effect on T currents and $GABA_A$ receptors, in vivo analgesia showed strong enantioselectivity. The lower panel of Fig. 4A shows that the dose-dependent prolongation of PWLs is of smaller magnitude with *ent*-3α5αP (maximal increase of 3.6 s with 3 μg/100 μL) than with 3α5αP (maximal increase of about 6 s with 1 μg/100 μL). Fig. 4B compares the increase in difference between injected (right paw) and non-injected (left paw) PWLs as a function of increasing 3α5αP (closed circles) or *ent*-3α5αP (open circles) doses when measured at peak effect (10 min post-injection). Both 3α5αP and *ent*-3α5αP induced dose-dependent peripheral analgesia but 3α5αP was more potent (an ED_{50} of 0.01 ± 0.002 μg/100 μL for 3α5αP and an ED_{50} of 0.05 ± 0.001 μg for *ent*-3α5αP) in addition to inducing higher maximal prolongation of PWLs. The dose–response curve for *ent*-3α5αP was shifted five-fold to the right when compared to 3α5αP.

To compare analgesic properties of 3α5αP with other neuroactive steroids that have similar mechanisms of action, we performed in vitro and in vivo experiments using two additional pairs of 5α-reduced neuroactive steroid enantiomers: (1) ALPX, a prototypical 5α-reduced neuroactive steroid and anesthetic with analgesic properties as documented in animal (Gilron and Coderre, 1996) and human studies (Sear, 1996) and its enantiomer, *ent*-ALPX; and (2) ACN and its enantiomer *ent*-ACN (Wittmer et al., 1996).

ALPX potently enhanced GABA currents with a threshold for activity near 0.1 μM ($74\pm9\%$ potentiation; $n=4$) and near maximum potentiation at 10 μM ($2900\pm498\%$ potentiation; $n=4$) on recombinant receptors expressed in Xenopus oocytes (data not shown). *Ent*-ALPX had no detectable effect on GABA responses at 0.1 or 1 μM but yielded detectable potentiation at 10 μM ($161\pm19\%$; $n=4$) (data not shown). We previously reported that ALPX blocks isolated T currents in acutely dissociated rat sensory neurons (Todorovic et al., 1998). Here, we show that *ent*-ALPX partially blocks isolated DRG T currents (maximal block of about 60%) in a concentration-dependent manner (Fig. 5, top panel). *Ent*-ALPX was substantially less potent than ALPX in blocking T currents even when applied to the same cell (Fig. 5, middle panel). Consequently, the concentration–response curve for *ent*-ALPX (solid line) was shifted to the right about 20-fold when compared to the concentration–response curve for ALPX (dashed line) (Fig. 5, lower panel). The calculated IC_{50} for *ent*-ALPX-induced blockade of T currents in rat sensory neurons was 29.0 ± 0.6 μM. We previously reported that the calculated IC_{50} for ALPX-induced blockade of T currents in rat sensory neurons was 1.3 ± 0.3 μM (Todorovic et al., 1998).

In vivo experiments demonstrate that ALPX induced dose-dependent and potent analgesia when injected locally into peripheral receptive fields of sensory neurons (Fig. 6, upper panel). Significant analgesia was achieved with very low doses of ALPX (as low as 0.03 μg/100 μL).

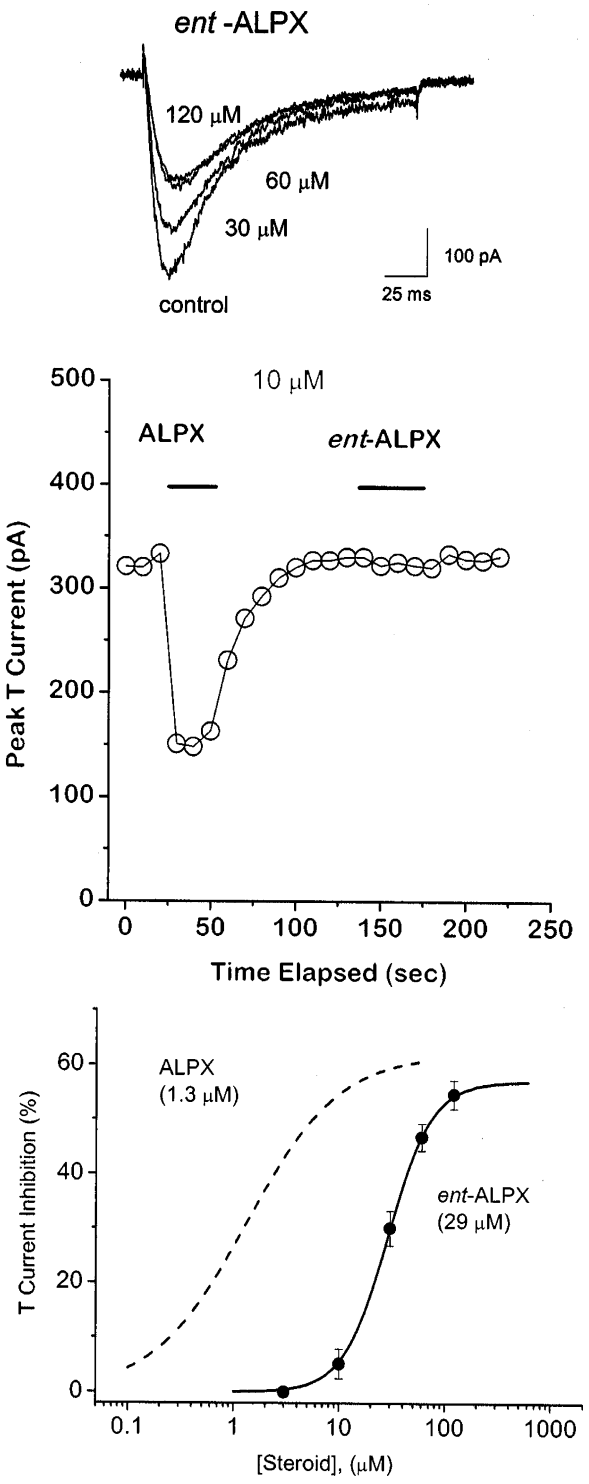

Fig. 5. ALPX is potent and enantioselective blocker of T currents in small size rat sensory neurons. *Upper panel*—Leak-subtracted traces from an experiment where escalating concentrations (from 30 to 120 μM) of *ent*-ALPX were applied to the same cell. Note that the application of 120 μM of *ent*-ALPX induced very little additional blockade of T current compared to T current blockade recorded with 60 μM. Currents were elicited by stepping the membrane potential from −90 to −35 mV. Bars indicate calibration. *Middle panel*—The time course of T current blockade obtained from a separate experiment where the effects of ALPX and *ent*-ALPX were recorded from the same cell. During the application of 10 μM ALPX, as indicated by horizontal bars, a peak T current was transiently decreased (by about 57%). However, at this concentration, *ent*-ALPX had very little effect on T-current. *Lower panel*—The graph shows the concentration-dependent blockade of T currents by ALPX and *ent*-ALPX. Points represent averages of at least five different cells, vertical lines represent standard errors (SE) and solid line is the best fit of the Hill equation yielding an IC_{50} value of 29±1 μM with Hill coefficient of 2.1±0.1 and maximal block of 57±1 (total of 12 cells) for *ent*-ALPX. Dashed line is the best fit of the Hill equation yielding an IC_{50} value of 1.3±0.3 μM with Hill coefficient of 0.9±0.1 and maximal block of 62±5% for ALPX (from Todorovic et al., 1998).

The highest dose (1 μg/100 μL) induced profound analgesia (an increase in thermal PWLs of about 5 s when compared to non-injected paw at 10 min) that lasted at least 20 min. Stable PWLs recorded from the non-injected contra-lateral paw indicate lack of systemic effect. ALPX showed strong enantioselectivity in its peripheral analgesic effects. Although the maximal effect with *ent*-ALPX (an increase in thermal PWLs of about 5 s when compared to non-injected paw at 10 min) was similar to that achieved with ALPX, the maximum required dose of *ent*-ALPX was three-fold higher (3 μg/100 μL) (Fig. 6, middle panel). Fig. 6 (lower panel) shows the increase in difference between injected (right paw) and non-injected (left paw) PWLs as a function of increasing ALPX (open circles) and *ent*-ALPX (closed triangles) doses when measured at peak effect (10 min post-injection). Both ALPX and *ent*-ALPX induced dose-dependent peripheral analgesia, but *ent*-ALPX was about six-fold less potent (ED_{50} of 0.04±0.01 μg/100 μL for ALPX and ED_{50} of 0.23±0.09 μg/100 μL for *ent*-ALPX). This strong enantioselectivity of ALPX analgesia in vivo parallels the enantioselectivity of ALPX observed in the in vitro experiments (Fig. 5, lower panel). It is noteworthy that the analgesic potency of 3α5αP and ALPX is comparable to the potency of these two steroids in blocking T-currents in rat sensory neurons (i.e. 3α5αP is the more potent analgesic in vivo and the more potent blocker of T-current in rat sensory neurons in vitro).

ACN represents another 5α-reduced neuroactive steroid with mechanisms of action similar to 3α5αP and ALPX that has been shown to exhibit strong enantioselectivity in vitro. ACN is about 50 times more potent in blocking isolated T currents in rat sensory neurons than *ent*-ACN (IC_{50}s of 0.4 and 28 μM for ACN and *ent*-ACN, respectively) (Todorovic et al., 1998) and is similarly more potent in potentiating $GABA_A$ currents in hippocampal neurons (Wittmer et al., 1996) than *ent*-ACN. Fig. 7 compares peripheral analgesic effects of ACN and *ent*-ACN in vivo. ACN and *ent*-ACN induced dose-dependent peripheral analgesia when injected locally into peripheral receptive fields of sensory neurons. While significant analgesia was achieved with 0.1 μg/100 μL ACN, a three times higher dose of *ent*-ACN was needed to induce a similar analgesic response. The highest dose (3 μg/100 μL) of ACN induced more profound analgesia (an increase in thermal PWLs of about 5 s when

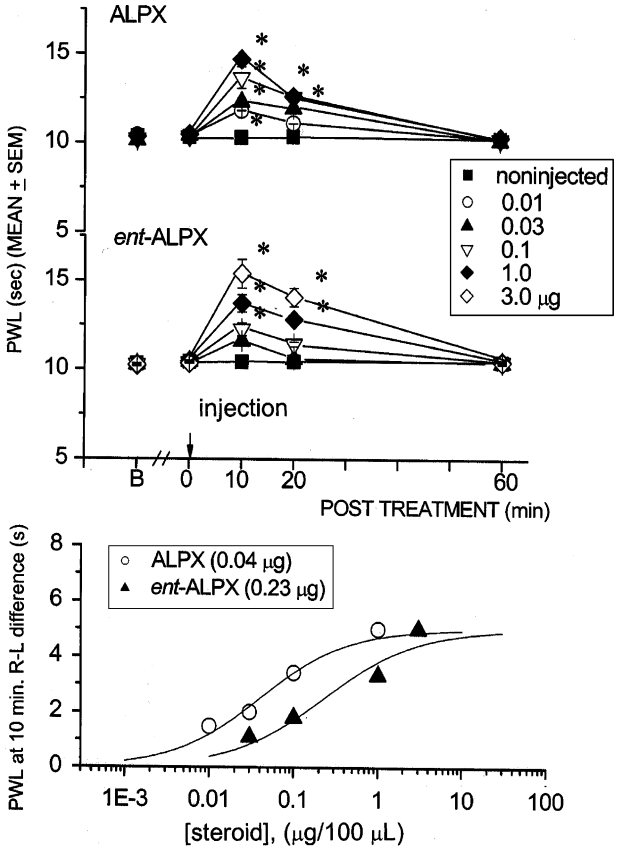

Fig. 6. ALPX is a potent and enantioselective peripheral analgesic. *Upper panel*—Injection of ALPX induces a dose-dependent increase in thermal PWLs when compared to non-injected paws. At 0.01, 0.03, 0.1 and 1.0 μg/100 μL, ALPX significantly increased PWLs [*, $F(1,4)=4.06$, $P<0.001$; $F(1,4)=12.95$, $P<0.0001$; $F(1,4)=14.75$, $P<0.0001$; $F(1,4)=18.59$, $P<0.0001$, respectively] at 10 min and the two highest doses (0.1 and 1.0 μg/100 μL) significantly increased PWLs [*, $F(1,4)=9.82$, $P<0.001$; $F(1,4)=6.28$, $P<0.001$, respectively] at 20 min post-injection when compared to the non-injected paw (closed squares). PWLs returned to control values by 60 min following injection ($n=9$–12 animals per time point). *Middle panel*—Injection of *ent*-ALPX induces a dose-dependent increase in thermal PWLs when compared to non-injected paws. At 0.1, 1.0, and 3.0 μg/100 μL, *ent*-ALPX significantly increased PWLs [*, $F(1,16)=28.41$, $P<0.0001$; $F(1,16)=52.23$, $P<0.0001$; $F(1,16)=41.68$, $P<0.0001$, respectively] at 10 min and significantly increased PWLs [*, $F(1,16)=43.33$, $P<0.0001$; $F(1,16)=202.32$, $P<0.0001$; $F(1,16)=51.71$, $P<0.0001$, respectively] at 20 min post-injection when compared to the non-injected paw (closed squares). PWLs returned to control values by 60 min following injection ($n=9$–12 animals per time point). *Lower panel*—Dose-dependent thermal analgesia following local injection of ALPX (open circles) and *ent*-ALPX (closed triangles). Average dose–response curves for local analgesia are based on the maximal increase in thermal PWLs on injected paw (right) vs. non-injected (left) paw 10 min after the injection (the maximal effect) (*y*-axis) and dose of ALPX or *ent*-ALPX expressed in μg/100 μL (*x*-axis). Solid lines are best fits of the Hill equation (see Section 2). Fits for both curves were constrained to maximal increase in PWLs of 5.0 s with $ED_{50}=0.04\pm0.01$ and 0.23 ± 0.09 μg, Hill coefficient 0.8 ± 0.2 and 0.8 ± 0.6 for ALPX and *ent*-ALPX, respectively.

compared to non-injected paw at 10 min) when compared to *ent*-ACN (an increase in thermal PWLs of about 3 s). As shown in Fig. 7 (lower panel), *ent*-ACN was a five-fold less potent analgesic (the ED_{50} of 1.0 ± 0.14 μg/100 μL) than

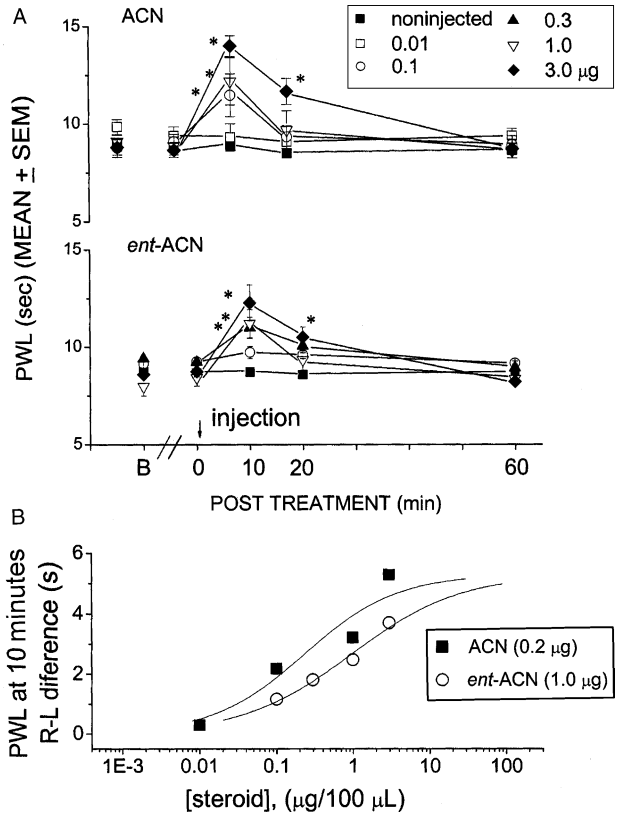

Fig. 7. The enantioselectivity of ACN-induced peripheral analgesia. *Upper panel*—Injection of ACN induces a dose-dependent increase in thermal PWLs when compared to non-injected paws. At 0.1,1.0 and 3.0 μg/100 μL, ACN significantly increased PWLs [*, $F(1,33)=5.35$, $P<0.05$; $F(1,33)=5.96$, $P<0.05$; $F(1,22)=86.86$, $P<0.0001$, respectively] at 10 min and the highest dose (3.0 μg/100 μL) significantly increased PWLs [*, $F(1,22)=19.72$, $P<0.0001$] at 20 min post-injection when compared to the non-injected paw (closed squares). PWLs returned to control values by 60 min following injection ($n=9$–12 animals per time point). *Middle panel*—Injection of *ent*-ACN induces a dose-dependent increase in thermal PWLs when compared to non-injected paws. At 0.3, 1.0, and 3.0 μg/100 μL, *ent*-ACN significantly increased PWLs [*, $F(1,4)=5.83$, $P<0.001$; $F(1,4)=8.08$, $P<0.001$; $F(1,4)=8.07$, $P<0.001$, respectively] at 10 min and at the highest dose (3.0 μg/100 μL) significantly increased PWLs [*, $F(1,4)=4.28$, $P<0.001$] at 20 min post-injection when compared to the non-injected paw (closed squares). PWLs returned to control values by 60 min following injection ($n=9$–12 animals per time point). *Lower panel*—Dose-dependent thermal analgesia following local injection of ACN (closed squares) and *ent*-ACN (open circles). Average dose–response curves for local analgesia are based on the maximal increase in thermal PWLs on injected paw (right) vs. non-injected (left) paw 10 min after the injection (the maximal effect) (*y*-axis) and dose of ACN or *ent*-ACN expressed in μg/100 μL (*x*-axis). Solid lines are best fits of the Hill equation (see Section 2). Fits for both curves were constrained to maximal increase in PWLs of 5.3 s with $ED_{50}=0.2\pm0.1$ and 1.0 ± 0.1 μg, Hill coefficient 0.7 ± 0.3 and 0.6 ± 0.1 for ACN and *ent*-ACN, respectively.

ACN (ED_{50} of 0.2 ± 0.14 μg/100 μL). It is important to note that the enantioselectivity of ACN analgesia in vivo parallels the enantioselectivity of ACN previously reported using in vitro systems (i.e. ACN is a more potent analgesic than *ent*-ACN in vivo and is more potent than *ent*-ACN in blocking T-currents and potentiating GABA-induced currents in vitro) (Todorovic et al., 1998; Wittmer et al., 1996).

Based on the in vivo findings, 3α5αP, ALPX and ACN are potent peripheral analgesics. However, because they have dual effects on T-type Ca^{2+} currents and GABA-induced currents over the same concentration range (Todorovic et al., 1998; Wittmer et al., 1996) it is difficult to determine whether their analgesic effects are mediated by $GABA_A$ receptors or T-channels (or both). To begin to address this issue, we evaluated a recently described 5α-reduced neuroactive steroid analogue that has a novel structure, CDNC24, for its actions on T currents. This pentacyclic cyclodinorcholene steroid is a potent enhancer of GABA-mediated currents (similar in potency to ALPX and 3α5αP) (Jiang et al., 2003), with little effect on T currents (Fig. 8, top panel). At 10 μM, which is the concentration that caused near maximal blockade of T current in rat sensory neurons when 3α5αP (Fig. 2D), ALPX (Fig. 6, lower panel) or ACN (Todorovic et al., 1998) were applied, CDNC24 had very little effect on T currents in rat sensory neurons in vitro (4±2% block, $P>0.05$; $n=6$ cells). However, at the same concentration, CDNC24 significantly potentiated $GABA_A$ currents (approximately 20-fold) (Fig. 8, middle panel). To assess whether a steroid that lacks effects on T-type Ca channels, but has potent GABAergic effects has analgesic properties, we performed in vivo studies with CDNC24 (Fig. 8, lower panel). We found that CDNC24, at 1 μg/100 μL had no effect on thermal PWLs. However, at this dose, ALPX, ACN and 3α5αP induced near-maximal increase in PWLs (Figs. 4, 6 and 7).

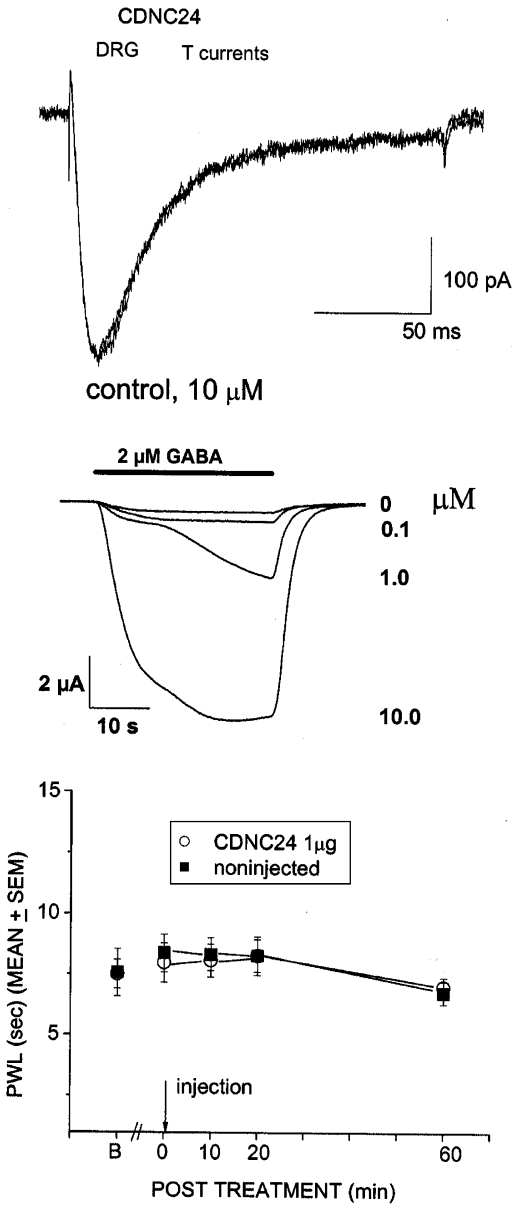

Fig. 8. A lack of effects of GABA-mimetic steroid, CDNC24, in peripheral nociception. *Top panel*—CDNC24, at 10 μM, has no effect on T-currents in dissociated rat sensory neurons in vitro. *Middle panel*—CDNC24 causes potent and concentration-dependent potentiation of GABA currents elicited by the application of 2 μM GABA in oocytes expressing recombinant rat α1β2γ2L type $GABA_A$ receptors in vitro. *Lower panel*—Local injection of CDNC24, at 1 μg/100 μL, had no effect on thermal nociception in vivo as indicated by the lack of difference between PWLs in injected vs. non-injected paws ($n=9$ animals per time point).

Furthermore, a competitive $GABA_A$ antagonist, bicuculline, in doses ranging from 0.3 to 3 μg/100 μL partially blocked, but failed to abolish ALPX-induced analgesia (doses of ALPX ranging between 0.3 and 1 μg/100 μL) ($n=9$ animals per dose, data not shown). These data strongly suggest that $GABA_A$ receptors play a limited role in peripheral anti-nociception induced by 5α-reduced neuroactive steroids.

To evaluate further the role of peripheral T-type Ca^{2+} channels in peripheral analgesia induced by 5α-reduced neuroactive steroids we used ECN, 5α-reduced neuroactive steroid that blocks T-channel currents in rat sensory neurons and, unlike many other neuroactive steroids, has no effect on $GABA_A$ currents (Todorovic et al., 1998). We have reported that ECN is about 30 times more potent in blocking isolated T currents in rat sensory neurons (IC_{50} 300 nM) (Todorovic et al., 1998) than *ent*-ECN. Fig. 9 compares peripheral analgesic effects of ECN and *ent*-ECN in vivo. Both enantiomers induced dose-dependent peripheral analgesia when injected locally into peripheral receptive fields of sensory neurons. While significant analgesia was achieved with 0.1 μg/100 μL of ECN, a 10 times higher dose of *ent*-ECN (1.0 μg/100 μL) was needed to induce significant analgesic responses. However, the maximal analgesic effect induced by the highest doses of ECN and *ent*-ECN (3 μg/100 μL) was similar (about 3 sec increase in PWLs at 10 min post-injection). As shown in Fig. 9 (lower panel), ECN was a seven-fold more potent analgesic (the ED_{50} of 0.02±0.01 μg/100 μL) than *ent*-ECN (ED_{50} of 0.15±0.04 μg/ 100 μL). These data strongly suggest that potent analgesia induced by 5α-reduced neuroactive steroids, at least in part, results from blockade of T-type Ca^{2+} channels in peripheral nociceptors.

The in vivo data indicate that T-type Ca^{2+} channels play an important role in mediating potent peripheral

analgesia induced by 5α-reduced neurosteroids. This conclusion is based on the assumption that peripheral nerve endings of sensory neurons express a repertoire of ion channels similar to cell somas in DRG and the fact that the neurosteroid that is a potent blocker of T-channels (e.g. ECN) is also a potent analgesic in the in vivo study. In contrast, CDNC24, which has actions at $GABA_A$ receptors but not at T-channels was ineffective in inducing analgesia when injected alone in peripheral receptive fields. However, also note that all compounds that are both T-channel blockers and potentiators of $GABA_A$ currents in vitro (e.g. ACN, ALPX and 3α5αP), when studied in vivo, produced higher maximal prolongation of PWLs (about 5–6 s) than ECN (about 3 s) suggesting that $GABA_A$ receptors may also contribute to peripheral analgesia.

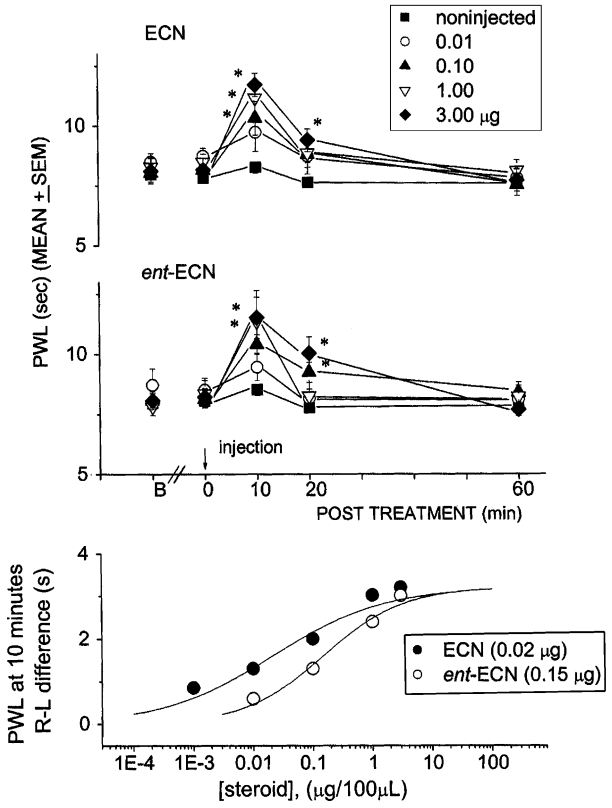

Fig. 9. Selective T-type Ca^{2+} channel blocker, ECN, causes enantioselective analgesia. *Upper panel*—Injection of ECN induces a dose-dependent increase in thermal PWLs when compared to non-injected paws. At 0.1,1.0 and 3.0 μg/100 μL, ECN significantly increased PWLs [*, $F(1,22)=18.18$, $P=0.000$; $F(1,22)=4.72$, $P<0.05$; $F(1,22)=24.94$, $P<0.0001$, respectively] at 10 min and the highest dose (3.0 μg/100 μL) significantly increased PWLs [*, $F(1,22)=7.43$, $P<0.012$] at 20 min post-injection when compared to the non-injected paw (closed squares). PWLs returned to control values by 60 min following injection ($n=9$–12 animals per time point). *Middle panel*—Injection of *ent*-ECN induces a dose-dependent increase in thermal PWLs when compared to non-injected paws. At 1.0, and 3.0 μg/100 μL, *ent*-ECN significantly increased PWLs [*, $F(1,22)=10.41$, $p=0.004$; $F(1,22)=20.64$, $P<0.0001$, respectively] at 10 min and significantly increased PWLs [*, $F(1,22)=7.72$, $P=0.001$; $F(1,22)=7.06$, $P=0.014$, respectively] at 20 min post-injection when compared to the non-injected paw (closed squares). PWLs returned to control values by 60 min following injection ($n=9$—12 animals per time point). *Lower panel*—Dose-dependent thermal analgesia following local injection of ECN (closed circles) and *ent*-ECN (open circles). Average dose–response curves for local analgesia are based on the maximal increase in thermal PWLs on injected paw (right) vs. non-injected (left) paw 10 min after the injection (the maximal effect) (*y*-axis) and dose of ECN or *ent*-ECN expressed in μg/100 μL (*x*-axis). Solid lines are best fits of the Hill equation (see Section 2). Fits for both curves were constrained to maximal increase in PWLs of 3.2 s with $ED_{50}=0.02\pm0.01$ and 0.15 ± 0.04 μg, Hill coefficient 0.5 ± 0.01 and 0.7 ± 0.1 for ECN and *ent*-ECN, respectively.

This led us to examine possible interactions between T-channels and $GABA_A$ channels in peripheral nociceptors in vivo by combining selective compounds for T-channel blockade (e.g. ECN) and $GABA_A$ channel potentiation (e.g. CDNC24). Fig. 10A (upper panel) shows that, when these two agents were combined, 1.0 μg/100 μL of CDNC24 that was co-injected with increasing doses of ECN greatly enhanced the maximal analgesic response to all doses of ECN at 10 and 20 min following injections in peripheral receptive fields (compared to Fig. 9, upper panel). This potentiating effect of CDNC24 was completely abolished when 0.3 μg/100 μL bicuculline was co-injected with ECN and CDNC24 (lower panel, Fig. 10A). At this dose, when given alone, bicuculline did not significantly affect thermal PWLs ($n=9$ animals, data not shown). Fig. 10B summarizes the dose–response studies of $GABA_A$ and T-channels interactions. Although the ED_{50} for ECN analgesia measured 10 min after the injection was only slightly decreased by CDNC24 (from 0.020 to 0.015 μg/100 μL), the near-maximal response to 1 μg of ECN was almost doubled (from 3.2 s to 5.6 s) in the presence of CDNC24 (closed squares) ($P<0.01$). It is also evident that bicuculine, by blocking CDNC24-induced GABA potentiation, completely reversed the effect of CDNC24 on ECN-induced anti-nociception (open circles). Note that the dose–response curve to ECN alone (dotted line) nearly overlaps with the curve where bicuculline, ECN and CDNC24 were combined (solid line, open circles). To further study this issue we performed a series of experiments where the enhancement of ECN-induced analgesic response observed in the presence of CDNC24, at 1 μg/100 μL (Fig. 10A, upper panel), was compared with the enhancement observed in the presence of two lower doses of CDNC24 (0.3 μg/100 μl and 0.1 μg/100 μl). We found that CDNC24 augments the anti-nociceptive effects of ECN in dose-dependent fashion (i.e. CDNC24 was less effective at 0.3 than at 1 μg/100 μL in enhancing ECN-induced dose-dependent analgesic response, but was practically ineffective at 0.1 μg/100 μL) ($n=9$ animals for each experiment, data not shown). In conclusion, these data strongly suggest that T-channels, but not $GABA_A$ channels, contribute to baseline peripheral nociceptive signaling. However, enhancement of $GABA_A$ channel activity contributes to peripheral anti-nociception if T-channels are blocked simultaneously.

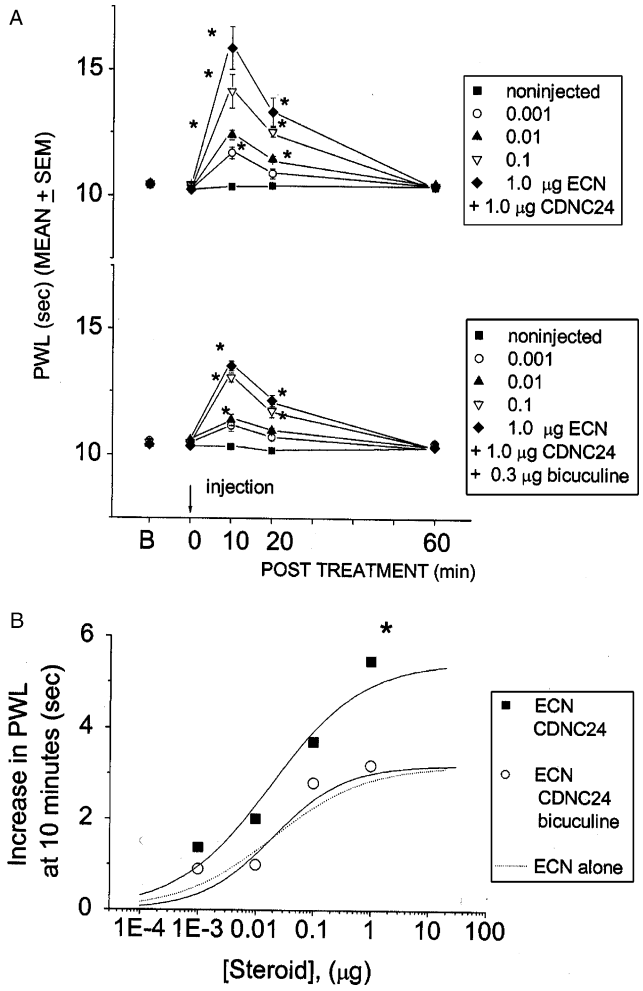

Fig. 10. Contribution of $GABA_A$ channels to peripheral analgesia mediated by 5α-reduced steroids. (A) *Upper panel*—Co-injection of CDNC24 (at 1.0 μg/100 μL) with various doses of ECN induces a dose-dependent increase in thermal PWLs when compared to non-injected paws. At all doses that were tested, 0.001, 0.01, 0.1 and 1.0 μg/100 μL, ECN in the presence of 1.0 μg/100 μL of CDNC24 significantly increased PWLs [*, $F(1,32)=8.44$, $P<0.001$; $F(1,32)=16.52$, $P<0.001$; $F(1,32)=12.87$, $P<0.001$, $F(1,32)=12.23$, $P<0.001$, respectively] at 10 min and at 0.01, 0.1 and 1.0 μg/100 μL significantly increased PWLs [*, $F(1,32)=8.5$, $P<0.001$; $F(1,32)=7.07$, $P<0.001$; $F(1,32)=6.65$, $P<0.001$] at 20 min post-injection when compared to the non-injected paw (closed squares). PWLs returned to control values by 60 min following injection ($n=9$–12 animals per time point). (A) *Middle panel*—Co-injection of CDNC24 (at 1.0 μg/100 μL)+bicuculine (at 0.3 μg/100 μL) with various doses of ECN induces a dose-dependent increase in thermal PWLs when compared to non-injected paws. At 0.01, 0.1 and 1.0 μg/100 μL, ECN in the presence of 1.0 μg/100 μL of CDNC24+0.3 μg/100 μL bicuculine significantly increased PWLs [*, $F(1,32)=7.87$, $P<0.001$; $F(1,32)=16.97$, $P<0.001$; $F(1,32)=23.56$, $P<0.001$, respectively] at 10 min and significantly increased PWLs [*, $F(1,32)=4.08$, $P<0.001$; $F(1,32)=7.67$, $P<0.001$; $F(1,32)=13.29$, $P<0.001$, respectively] at 20 min post-injection when compared to the non-injected paw (closed squares). PWLs returned to control values by 60 min following injection ($n=9$–12 animals per time point). (B) Dose-dependent thermal analgesia following local injections of various doses of ECN+1.0 μg/100 μL CDNC24 without (closed squares) or with 0.3 μg/100 μL bicuculine (open circles). Average dose–response curves for local analgesia are based on the maximal increase in thermal PWLs on injected paw (right) vs. non-injected (left) paw 10 min after the injection (the maximal effect) (*y*-axis) and dose of ECN with CDNC24 or with CDNC24+bicuculine. Solid lines are best fits of the Hill equation (see Section 2). Fits were constrained maximal increase in PWLs of 5.5 and 3.2 s with $ED_{50}=0.015\pm0.01$ and 0.01 ± 0.001 μg, Hill coefficient 0.54 ± 0.15 and 0.7 ± 0.2 for ECN+CDNC24 without and with bicuculine, respectively. Note that dotted line indicated dose–response to ECN alone. (*, $P<0.01$).

4. Discussion

4.1. Contribution of T-channels and $GABA_A$ receptors in peripheral nociception

In this study we demonstrate that 5α-reduced neuroactive steroids are potent peripheral analgesics. Structural modifications that eliminate blocking effects on T-type Ca^{2+} channels but preserve potentiation effects at $GABA_A$ receptors result in complete loss of steroid-induced analgesic activity. Thus, CDNC24, a steroid that potently enhances $GABA_A$ receptors but lacks effects on T currents, is an ineffective analgesic in comparison to ECN, a steroid that lacks $GABA_A$ receptor activity, but is a potent blocker of T currents (Todorovic et al., 1998). ECN was one of the most effective peripheral analgesics in this study. Additionally, the competitive $GABA_A$ antagonist, bicuculline, failed to completely block peripheral analgesia induced by ALPX, a potent neuroactive steroid with effects on both $GABA_A$ receptors and T-channels.

Although $GABA_A$ receptors are thought to play a role in centrally mediated analgesic effects of neuroactive steroids (Nadeson and Goodchild, 2000), our findings strongly suggest that their peripheral analgesic action is mediated primarily by T-channels and only to a smaller extent by $GABA_A$ receptors. Previous immunohistological studies have demonstrated $GABA_A$ channels on small nociceptive fibers in the skin. However, local application of muscimol, a $GABA_A$ agonist, into peripheral receptive fields of sensory neurons did not change thermal PWLs (Carlton et al., 1999). This is consistent with results obtained with the GABAergic steroid CDNC24. However, our experiments using a combination of ECN and CDNC24 strongly suggest that $GABA_A$ channels may contribute to steroid analgesia if T-channels are simultaneously blocked. A possible explanation for this finding is that intracellular Ca^{2+} may have a permissive role in controlling $GABA_A$ channel function in peripheral nociceptors, which could be achieved by Ca^{2+}-dependent modulatory pathways that tonically inhibit $GABA_A$ channels. Therefore, when voltage-dependent Ca^{2+} channels are blocked causing a decrease in intracellular Ca^{2+}, $GABA_A$ channels may be disinhibited and contribute to peripheral anti-nociception. We propose that there is a contribution of both T-channels and $GABA_A$ channels to steroid-induced peripheral antinociception and that steroids that have effects on both systems (e.g. ACN, 3α5αP and ALPX) may have 'built-in' analgesic efficacy by blocking T-channels and potentiating currents mediated by $GABA_A$ channels. Our studies with steroid analogues that

uncouple effects on $GABA_A$ and T-type Ca^{2+} channels reveal a novel role of $GABA_A$ channels in peripheral nociception.

4.2. T-type Ca^{2+} channels in peripheral nociceptors as targets for steroid-induced analgesia

Although the presence of T-channels was initially described in nociceptors (e.g. dorsal root ganglia neurons (Carbone and Lux, 1984), their role in peripheral nociception has only recently been demonstrated (Todorovic et al., 2001, 2002). Similarly, Kim et al. (2003) recently described a role of T-channels in visceral nociception. Studies examining the role of T-type Ca^{2+} channels in pain have been hampered by a lack of specific blockers that do not affect other voltage-gated ion channels. In vitro analysis of ECN has showed that this 5α-reduced steroid is a potent blocker of neuronal T-channels but has 30-fold less potent effect on HVA currents in rat sensory neurons and no effect on neuronal voltage-gated Na^+ and K^+ channels at concentrations that suppress T currents (Todorovic et al., 1998). ALPX is also a potent inhibitor of T currents with no effect on HVA currents in rat sensory neurons in concentrations up to 10 μM, and block of Na^+ and K^+ currents only at very high concentrations (80–300 μM) (Benoit et al., 1988). Interestingly, the plasma concentrations of ALPX required for achieving analgesia in humans range from 6 to 13 μM (Sear and Prys-Roberts, 1979), suggesting that T-type channels are blocked by ALPX at clinically relevant concentrations. Similarly, ACN and 3α5αP, steroids that are potent peripheral analgesics are much more potent in blocking T-channels than HVA channels in sensory neurons (Todorovic et al., 1998; Nakashima et al., 1998). Similarly we previously reported that 3α5αP does not affect neuronal HVA Ca^{2+} currents at concentrations up to 10 μM (Nakashima et al., 1998) and we report here no effect of this concentration of 3α5αP on voltage-gated Na^+ and K^+ currents. Assuming that similar ion channels exist in cell soma and nerve terminals, these findings strongly suggest that the analgesic effects of 5α-reduced neuroactive steroids observed in vivo likely result from modulation of T-type Ca^{2+} currents in peripheral nociceptors and not from modulation of other voltage-gated ion currents.

Our studies demonstrate that blockade of T currents by 5α-reduced neuroactive steroids exhibits strong enantioselectivity (Todorovic et al., 1998). Here we also show that this enantioselectivity parallels their analgesic effects in vivo. Steroid enantiomers that have the absolute configuration of naturally occurring steroids are more potent blockers of T currents than their non-naturally occurring enantiomers in vitro, and are also more potent peripheral analgesics in vivo. This suggests that the site affected by these steroids in sensory neurons and peripheral nociceptors is similar and has specific structural requirements. Additionally, recent studies of the interactions of cholesterol, a steroid known to have major effects on cell membranes, with model membrane lipids have shown that cholesterol/lipid interactions are not enantioselective (Mannock et al., 2003; Westover et al., 2003). Hence, the enantioselectivity shown here strongly suggests that 5α-reduced neuroactive steroids do not induce analgesia simply by causing non-specific perturbation of lipid membranes in peripheral nociceptors.

It is interesting that this study and our previous study of 5α-reduced steroids showed that these compounds induce only a partial block of T currents. We showed that 3α5αP induced a mild voltage-dependent block with a shift of V_{50} about 10 mV (Fig. 3) similar to ECN, ACN and ALPX (Todorovic et al., 1998). This mild voltage-dependence of block indicates preference of steroids for inactive states of the channel and could contribute to partial block at certain voltages. Notably, inhibition was apparent even at the most deeply negative membrane potentials (Fig. 3), indicating a shift in V_{50} is not the only effects of steroids. Partial block could also result from involvement of unidentified second messengers, allosteric modulation, presence of accessory subunits of T-channel in DRG cells and/or preferential block of a particular isoform of T-channel expressed in DRG cells. Allosteric modulation is usually accompanied by changes in current kinetics and second messenger-mediated response often exhibit characteristic desensitization. We did not observe desensitization of responses or kinetic changes of T current associated with the blocking effect of steroids in our studies. It is important to note that some other clinically important agents such as anticonvulsants, phenytoin and valproic acid, also induce only partial block of T current in DRG cells as well as recombinant $Ca_V3.2$ channels in HEK cells without shifting the voltage dependence of inactivation (Todorovic et al., 1998, 2000). Thus, the reason for the partial block of T currents by neurosteroids and anticonvulsants in DRG cells remains unknown.

4.3. Neuroactive steroids as novel therapeutic agents for pain management

Direct application of 5α-reduced neuroactive steroids in peripheral receptive fields of cutaneous nociceptors results in significant analgesia to acute thermal stimuli. The doses of locally applied steroids that achieve significant analgesia make 5α-reduced steroids among the most potent peripheral analgesics yet described. Our data suggest that peripherally applied 5α-reduced neuroactive steroids could be useful therapeutic agents in conditions associated with acute cutaneous thermal nociception such as chemical/thermal burns, surgical thermo-coagulation and/or sunburns. These steroids are potent and highly lipid soluble which makes them readily available at peripheral nerve endings. In addition, because most peripheral nociceptors are polymodal and respond to noxious chemical and

mechanical stimuli as well, peripherally applied 5α-reduced neuroactive steroids may be useful for the treatment of pain associated with other types of peripheral tissue injury (e.g. post-operative pain). It is noteworthy that the inhibition of T currents by 5α-reduced neuroactive steroids in vitro exhibits use- and voltage-dependence (Todorovic et al., 1998; this study), suggesting that the block might be more prominent in conditions associated with peripheral tissue injury when nociceptive fibers are at heightened levels of activity.

Acknowledgements

This study was supported by the Career Development Awards, K08-DA00428 (to S.M.T.) and K08-DA00406 (to V.J.-T.) from NIDA, NIH grant AG 11355 (to V.J.-T.), NIH grant GM 47969 (to D.F.C and C.F.Z.), NIH grants NS 40488 and AA 12952 (S.M.), the Bantly Foundation (C.F.Z.), and the Klingenstein Foundation (S.M.). V.J.-T. is an Established Investigator of the American Heart Association.

References

Benoit E, Carratu MR, Mitolo-Chieppa D. Interactions between molecules of a steroid anesthetic (alphaxalone) and ionic channels of nodal membrane in voltage-clamped myelinated nerve fibre. Br J Pharmacol 1988;94(3):635–46.

Callachan H, Cottrell GA, Hather NY, Lambert JJ, Nooney JM, Peters JA. Modulation of the $GABA_A$ receptor by progesterone metabolites. Proc R Soc London B Biol Sci 1987;231(1264): 359–69.

Carbone E, Lux HD. A low-voltage activated, fully inactivating Ca channel in vertebrate sensory neurons. Nature 1984;310:501–2.

Cardenas CG, Del Mar LP, Scroggs RS. Variation in serotonergic inhibition of calcium channel currents in four types of rat sensory neurons differentiated by membrane properties. J Neurophysiol 1995;74: 1870–9.

Carlton SM, Zhou S, Coggeshall RE. Peripheral GABA(A) receptors: evidence for peripheral primary afferent depolarization. Neuroscience 1999;93:713–22.

Dogrul A, Gardell LR, Ossipov MH, Tulunay FC, Lai J, Porecca F. Reversal of experimental neuropathic pain by T-type calcium channel blockers. Pain 2003;(1/2):159–68.

Ertel SI, Ertel EA, Clozel JP. T-type Ca^{2+} channels and pharmacological blockade: potential pathophysiological relevance. Cardiovasc Drugs Ther 1997;11(6):723–39.

Gilron I, Coderre TJ. Preemptive analgesic effects of steroid anesthesia with alphaxalone in the rat formalin test. Evidence for differential GABA(A) Receptor modulation in persistent nociception. Anesthesiology 1996;84(3):572–9.

Han M, Zorumski CF, Covey DF. Neurosteroid analogues. 4. The effect of methyl substitution at the C-5 and C-10 positions of neurosteroids on electrophysiological activity at $GABA_A$ receptors. J Med Chem 1996; 39:4218–32.

Hargreaves K, Dubner R, Brown F, Flores C, Joris J. A new and sensitive method for measuring thermal nociception in cutaneous hyperalgesia. Pain 1988;32:77–88.

Hu Y, Zorumski CF, Covey DF. Neurosteroid analogues: structure–activity studies of benz[e]indene modulators of $GABA_A$ receptor function. 1. The effect of 6-methyl substitution on the electrophysiological activity of 7-substituted benz[e]indene-3-carbonitriles. J Med Chem 1993;36: 3956–67.

Hu Y, Wittmer LL, Kalbrenner M, Evers AS, Zorumski CF, Covey DF. Neurosteroid analogues. 5. Enantiomers of neuroactive steroids and benz[e]indenes: total synthesis, electrophysiolgical effects on $GABA_A$ receptor function and anesthetic action in tadpoles. J Chem Soc Perkin Trans 1997;I:3665–71.

Huguenard JR. Low-threshold calcium currents in central nervous system neurons. Annu Rev Physiol 1996;58:329–48.

Jevtovic-Todorovic V, Wozniak DF, Powell S, Nardi A, Olney JW. Clonidine potentiates the neuropathic pain-relieving action of MK-801 while preventing its neurotoxic and hyperactivity side effects. Brain Res 1998;781:202–11.

Jevtovic-Todorovic V, Meyenburg AP, Olney JW, Wozniak DF. Anti-parkinsonian agents procyclidine and ethopropazine alleviate thermal hyperalgesia in neuropathic rats. Neuropharmacology 2003;44: 739–48.

Jiang X, Manion BD, Benz A, Rath NP, Evers AS, Zorumski CF, Mennerick S, Covey DF. Neurosteroid analogues. 9. Conformationally constrained pregnanes: structure–activity studies of 13,24-cyclo-18, 21-dinorcholane analogues of the GABA modulatory and anesthetic steroids (3alpha, 5 alpha)- and (3alpha,5beta)-3-hydroxypregnan-20-one. J Med Chem 2003;46(25):5334–48.

Kim D, Park D, Choi S, Lee S, Sun M, Kim C, Shin H-S. Thalamic control of visceral nociception mediated by T-type Ca^{2+} channels. Science 2003;302(2):117–9.

Lambert JJ, Belelli D, Hill-Venning C, Peters JA. Neurosteroids and $GABA_A$ receptor function. Trends Pharm Sci 1995;16:295–303.

Majewska MD, Harrison NL, Schwartz RD, Barker JL, Paul SM. Steroid hormone metabolites are barbiturate-like modulators of the GABA receptor. Science 1986;232(4753):1004–7.

Mannock DA, McIntosh TJ, Jiang X, Covey DF, McElhaney RN. Effects of natural and enantiomeric cholesterol on the thermotropic phase behavior and structure of egg sphingomyelin bilayer membranes. Biophys J 2003;84(2 Pt 1):1038–46.

Nadeson R, Goodchild CS. Antinociceptive properties of neurosteroids II. Experiments with Saffan and its components alphaxalone and alphadolone to reveal separation of anaesthetic and antinociceptive effects and the involvement of spinal cord GABA(A) receptors. Pain 2000;88(1):31–9.

Nakashima YM, Todorovic SM, Covey DF, Lingle CJ. The anesthetic steroid (+)-3α-hydroxy-5α-androstane-17β-carbonitrile blocks N-, Q-, and R-type, but not L- and P-type, high voltage-activated Ca^{2+} current in hippocampal and dorsal root ganglion neurons of the rat. Mol Pharmacol 1998;54:559–68.

Perez-Reyes E. Molecular physiology of low-voltage-activated T-type calcium channels. Physiol Rev 2003;83:117–61.

Schroeder JE, Fischbach PS, McCleskey EW. T-type calcium channels: heterogeneous expression in rat sensory neurons and selective modulation by phorbol esters. J Neurosci 1990;10:947–51.

Sear JW. Steroid anesthetics: old compounds, new drugs. J Clin Anesth 1996;8(3 Suppl):91S–98.

Sear JW, Prys-Roberts C. Plasma concentrations of alphaxalone during continuous infusion of Althesin. Br J Anaesth 1979;51(9): 861–5.

Todorovic SM, Lingle CJ. Pharmacological properties of T-type Ca^{2+} current in adult rat sensory neurons: effects of anticonvulsants and anesthetic agents. J Neurophysiol 1998;79:240–52.

Todorovic SM, Prakriya M, Nakashima YM, Nilsson KR, Han M, Zorumski CF, Covey DF, Lingle CJ. Enantioselective blockade of T-type Ca^{2+} current in adult rat sensory neurons by a steroid that lacks γ-aminobutyric acid-modulatory activity. Mol Pharm 1998;54: 918–27.

Todorovic SM, Perez-Reyes E, Lingle CJ. Anticonvulsants but not general anesthetics have differential blocking effects on different T-type current variants. Mol Pharmacol 2000;58:98–108.

Todorovic SM, Jevtovic-Todorovic V, Meyenburg A, Mennerick S, Perez-Reyes E, Romano C, Olney JW, Zorumski CF. Redox modulation of T-type calcium channels in rat peripheral nociceptors. Neuron 2001;31: 75–85.

Todorovic SM, Meyenburg A, Jevtovic-Todorovic V. Mechanical and thermal antinociception in rats following systemic administration of mibefradil, a T-type calcium channel blocker. Brain Res 2002;951: 336–40.

Westover EJ, Covey DF, Brockman HL, Brown RE, Pike LJ. Cholesterol depletion results in site-specific increases in epidermal growth factor receptor phosphorylation due to membrane level effects. Studies with cholesterol enantiomers. J Biol Chem 2003; 278(51):51125–33.

White G, Lovinger DM, Weight FF. Transient low-threshold Ca^{2+} current triggers burst firing through an afterdepolarizing potential in an adult mammalian neuron. Proc Natl Acad Sci USA 1989;86: 6802–6.

Wittmer LL, Hu Y, Kalkbrenner M, Evers AS, Zorumski CF, Covey DF. Enantioselectivity of steroid-induced $GABA_A$ receptor modulation and anesthesia. Mol Pharmacol 1996;50:1581–6.

Zorumski CF, Mennerick S, Isenberg KE, Covey DF. Potential clinical uses of neuroactive steroids. Curr Opin Investig Drugs 2000;1(3): 360–9.